J. Water Environ. Nanotechnol., 8(3): 241-253 Summer 2023

ORIGINAL RESEARCH PAPER

The GO-Fe_3O_4 /Psf Membrane Prepared by Phase Inversion for Filtration: Dyes and NaCl in Water

Munasir Nasir [1,*], Yekti Purnama Utami [1], Nuhaa Faaizatunnisa [2], Lydia Rohmawati [1], Evi Suebah [1], Ahmad Taufiq [3] and Ezza Syuhada Sazali [4]

[1]Department of Physics, Faculty of Mathematics and Sciences, Universitas Negeri Surabaya (Unesa), Indonesia
[2]Department of Chemistry, Faculty of Science and Analytical Data, Institut Teknologi Sepuluh Nopember (ITS), Surabaya, Indonesia
[3]Department of Physics, Faculty of Mathematics and Sciences, Universitas Negeri Malang (UM), Indonesia
[4]Department of Physics, Faculty of Science, Universiti Teknologi Malaysia (UTM), Malaysia

Received: 2023-02-01 Accepted: 2023-04-24 Published: 2023-08-09

ABSTRACT
This study aims to determine the effectiveness of the GO- Fe_3O_4/Psf membrane in filtering water contaminated with dyes and salt. The membrane was prepared using the phase inversion method, with variations in the composition of GO- Fe_3O_4 (0.25%, 0.50%, 0.75%, and 1.00%), with polysulfone as the polymer material and NMP as a diluent. The dead-end filtration method is used to study the ability to repel dyes and salt molecules in water and hydrophilicity (surface contact angle test) and morphology (SEM) to confirm the membrane profile. Furthermore, rejection and filtration performance tests were carried out on water contaminated with dye (methylene blue) and water containing salt through salt rejection, flow flux, and UV-VIS tests. The filtration test results showed that the membrane with a composition of 0.75% had a salt rejection percentage of 59.33% (the highest), and the lowest flow flux was 54.42 $L.m^{-2}.h^{-1}$. The dye filtering results (MB) demonstrated better performance on the same membrane. It has been observed that the permeate is brighter than the other membranes. These results indicate that the membrane with a GO- Fe_3O_4 concentration of 0.75 wt.% is the most effective compared to other membranes in filtering water. The presence of Fe3O4 nanoparticles increases the efficiency and durability of graphene membranes in salt rejection by increasing the surface charge and selectively adsorbing salt ions.

Keywords: Graphene, GO-Fe_3O_4 /Psf, Filtration, Membrane, Desalination

How to cite this article
Nasir M., Faaizatunnisa N., Rohmawati L., Suebah E., Taufiq A., Syuhada Sazali E., The GO-Fe_3O_4 /Psf Membrane Prepared by Phase Inversion for Filtration: Dyes and NaCl in Water, J. Water Environ. Nanotechnol., 2023; 8(3): 241-253.
DOI: 10.22090/jwent.2023.03.004

INTRODUCTION

Clean water is essential for human domestic, industrial, and agricultural needs. The current increase in population and industry has harmed environmental quality, as indicated by the decreasing water catchment area. The lack of water catchment areas has resulted in reduced raw water availability. Raw water now covers only 3% of the total water on Earth, while the remaining 97% is seawater [1]. Seawater consists of 96.5% pure water and has an average salt content of 3.5%. The salt content of seawater comes from mineral salts found in rocks and soil. Examples are sodium, potassium, and calcium [2].

Based on these facts, desalination is the most appropriate way to purify seawater [3]. Desalination is a process carried out to remove salt levels [4]. Desalination can take advantage of phase changes or involve a semipermeable membrane to separate solutes[3]. The desalination process has been widely used in membrane technology [5] due to its low production cost [6], fewer chemicals [7], and energy usage, and is simple and environmentally

* Corresponding Authors Email: *munasir_physics@unesa.ac.id*

friendly [3]. In addition, membrane technology is very selective of the pore size so that only molecules smaller than the membrane pore size pass during the filtration process [8]. The membranes commonly used are microfiltration (MF), ultrafiltration (UF), and nanofiltration (NF) membranes [6].

Membranes that are often used for desalination are polymer membranes [7]. Polymer membranes have high flexibility [9] and good selectivity compared to inorganic membranes [10], but the low permeation performance of the membrane causes membrane fouling [9]. Combining polymer membranes and inorganic nanoparticles can overcome the problem of membrane fouling [7], [10]. Incorporating inorganic nanoparticles into the membrane matrix can improve membrane performance[7], such as hydrophilicity and membrane porosity, and minimize membrane fouling [11], [12]. Inorganic nanoparticles that are widely used are Fe_3O_4 or magnetic sand [10]. Magnetite (Fe_3O_4) is one of the strongest known iron dioxides of metals [13]. Fe_3O_4 nanoparticles are usually smaller than 128 nm [14]. Fe_3O_4 has good thermal stability, chemical stability, and magnetic properties [10]. In addition to their low toxicity and environmental friendliness, Fe_3O_4 nanoparticles have received much attention [7]. Fe_3O_4 can absorb both heavy metals such as Cr, Pb, Mn, Cu, etc. [14] and dyes such as methylene blue [15] in water. In addition, Fe_3O_4 can also be used in the separation of proteins or enzymes and DNA purification [16].

The incorporation of inorganic nanoparticles into the membrane matrix is always hindered by poor aggregation at higher levels [10]. This condition will harm the morphology and performance of the membrane in rejection, pure water flux, and hydrophilicity [7]. Nanohybrids can be a solution to avoid aggregation. A nanohybrid is a combination of two different nanoparticles. One of the materials frequently utilized in nanohybrids is graphene oxide (GO). The GO material exhibits a 2D nanostructure, a large surface area, and hexagonal chains [14], allowing different nanoparticles to bind to the GO surface [10]. Furthermore, GO has many functional groups containing oxygen (hydroxyl, epoxide, carbonyl, and carboxyl) which are good for nanofiller dispersion so that it can produce high effective surface area and good mechanical properties [7] and electrical and thermal properties [17]. In addition, the O-H bond in GO acts as a polarization center which can produce a greater absorbance intensity [16], [18].

GO-Fe_3O_4 material can be applied as a dye absorbent [19], dye degradation [14], and heavy metal reducer [20]. The PVDF-Fe_3O_4 membrane with 70 wt.% Fe_3O_4 has excellent comprehensive performance in pure water flux and good dirty resistance [11]. L. Donget al., studied GO/NH_2-Fe_3O_4 membranes and stated that GO/NH_2-Fe_3O_4 membranes could reject Congo red up to 94% and salt up to 15% [21]. Based on several studies that have been described, this research will discuss the effectiveness of the GO- Fe_3O_4 /PSf membrane in filtering water contaminated with natural dyes and seawater.

MATERIAL AND METHODS

Materials

The materials used to make the membrane were distilled water, graphite powder (from coconut shell), sodium nitrate powder ($NaNO_3$, Merck), potassium permanganate ($KMnO_4$), 30% hydrogen peroxide (30%, Merck), hydrochloric (HCl, fuming 37%, Merck), Aquades, 0.002 mol $FeCl_3.6H_2O$, Ammonia (NH_4OH) solution (28-30% Merck), and N-methyl-2-pyrrolidone (NMP, Merck), Polysulfon (Sigma-Aldrich).

Synthesis of Graphene (GO)

The Hummer method was used in this work to synthesize the graphene. Five grams of graphite powder and 2.5 grams of $NaNO_3$ powder were dissolved in 120 ml of H_2SO_4 in an ice bath (freezing point of water) and stirred using a magnetic stirrer for 30 minutes. Next, 15 grams of potassium permanganate was added slowly and stirred again for 30 minutes at 20°C until it became a purple solution, then continued stirring for 3 hours at room temperature. A brown solution was formed, and at that moment 150 mL of distilled water was added and stirred continuously for 3 hours at a room temperature of 95°C. Furthermore, 50 mL of 30% peroxide was added to a brownish-yellow (light brown) solution, added 50 mL of 30% peroxide was slowly to remove the manganate compound. In the final stage, the solution was washed with 1 M HCl, distilled to neutral (pH»7), and then dried for 6 hours at 60°C [21].

Synthesis of GO-Fe_3O_4 Composite

The GO-Fe_3O_4 composite was synthesized using the in-situ method. The GO powder was sonicated for 30 minutes in 100 ml of distilled water then

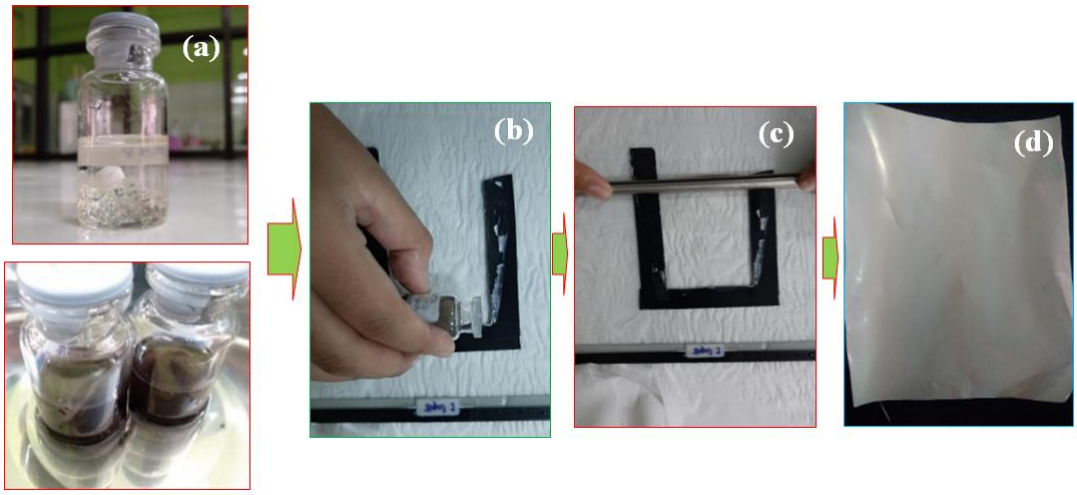

Fig. 1. Preparation of Psf, GO-Psf, and GO/Fe_3O_4-Psf membranes: (a) homogeneous solution, (b-c) membrane molding process, and (d) produced membrane.

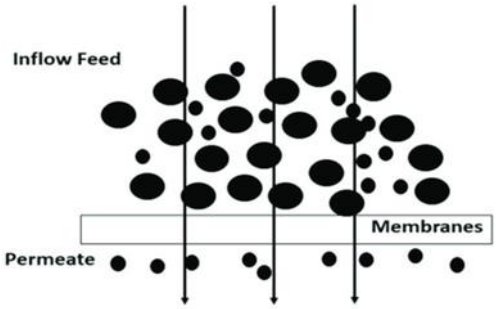

Fig. 2. Flow flux of permeate via membranes

0.002 moles of $FeCl_3.6H_2O$ was added and stirred until dissolved. Fe_3O_4 was formed simultaneously with the appearance of the GO-Fe_3O_4 composite. The solution was blackish-brown, then sonicated for one hour, and added 50 ml of 1.65 M Ammonia. The solution was washed with distilled water three times and dried for 3 hours at 600 °C.

Preparation of GO-Fe_3O_4 /PSf Membrane

The membrane was prepared using the phase inversion method. 15 wt.% Polly sulfones (Psf) were dissolved using 85 wt.% NMP (N-methyl-2-pyrrolidone) four hours until dissolve homogeneously. The next step is to add GO- Fe_3O_4 composite particle powder with a composition of 0.25 wt.%, 0.5 wt.%; 0.75 wt.% was then sonicated for 15 minutes to form a black homogeneous solution. The resulting solution was then printed on a glass plate with a thickness of 0.22 mm, which was rolled using an aluminum rod. The membrane was immersed in distilled water for 24 hours and dried at room temperature for 24 hours [22].

Methods

There are several methods to test filtration for NaCl and MB. Here are some methods used in this work.

Membrane Filtration Test for NaCl Solution

Synthetic seawater was prepared using distilled water with a NaCl concentration of 27.79 g/mL. The membrane was prepared with the sides measuring 3.5 cm x 3.5 cm (square shape); Later on, the membrane was tested for its filtration performance using a vacuum pump, with the device settings shown in Fig. 1. Before the filtration test, measure the mass of the membrane first and then put it in a Buchner funnel with a tapered side so that the solution does not seep through the side of the membrane. The Buchner funnel is then placed in a suction flask connected to a vacuum pump. In the filtration test, 10 ml of seawater was poured over the Buchner funnel and subsequently, the Rocker 300 vacuum pump was turned on with a vacuum

pressure of »650 mmHg. A bottle is used to store permeate that passes filtering. Once completed, the membrane filtration process is dried and weighed again.

Membrane Filtration Test for Dyes

20 ppm MB solution was prepared. A vacuum pipe tested the membrane of 3.5 cm x 3.5 cm (the shape of the membrane was a square) for filtration. The membrane was placed in a Buchner funnel with the side tapered to make the solution not come out from the side of the membrane when filtered. The Buchner funnel is then placed on a suction flask connected to a vacuum pipe. First, 10 ml of MB solution was poured over a Buchner funnel, and at that point, the Rocker 300 vacuum pump was turned on. The pressure was kept constant at 650 mmHg. The filtered methylene blue solution was poured into a small bottle and labeled.

Salt Rejection Test on Membrane

The salt-rejection test, often known as salt rejection, determines how much the membrane can filter NaCl compounds. The effectiveness of the membrane in separating salt depends on the size of the membrane pores. The following formula could be used to determine salt rejection [19], [20]:

$$Salt\ Rejection\ (\%) = \frac{C_p - C_f}{C_p} \times 100\% \quad (1)$$

Where C_p (mg/L) and C_f (mg/L) are a concentration of dyes and salts in permeate and feed solution, respectively.

Flow Flux of Membrane Filtration

The membrane flux test determines the parameters for membrane optimization. Low flux values indicate low membrane permeability. Flow flux calculations were performed in 10 ml of seawater (NaCl, 37%) or utilizing methylene blue at a pump pressure of 650 *mmHg* and a membrane surface area of 12.25 cm^2. The dead-end filtration model is a technique for separating particles or molecules from a solution by using a porous membrane that is forced through the solution to be separated. As the solution flows through the membrane, particles or molecules larger than the membrane's pore size will be suspended above the membrane, while the smaller solutes will pass through the membrane and exit the system [23].

$$J = \frac{V}{A \times t}\ (L.m^{-2}.h^{-1}) \quad (2)$$

Ultra Violet-Visible Spectroscopy

The filtered methylene blue solution will undergo by UV-Vis test (Shimadzu 1800 type) with a 200 nm to 600 nm wavelength. UV-VIS light will be passed through a methylene blue solution. Some of the light was absorbed (absorption) effectively and will be transmitted (transmitted). The absorbance value depends on the content of the substance in the solution. The more substances contained in the solution, the more molecules will absorb light, causing the absorbance value to be even greater [16], [21]. The results of UV-VIS measurements can be presented in the form of absorption spectra in the form of hills or transmission.

RESULT AND DISCUSSION

The hydrophilicity of Graphene Membrane

The hydrophilic property of the membrane plays an essential role in filtration performance. In principle, the hydrophilicity of the membrane could be determined by the water contact angle. The lower the contact angle, the higher the membrane hydrophilicity [24], [25]. The water contact angle results for pure Psf, GO-Fe_3O_4/Psf, and GO/Psf membranes with various Go-Fe_3O_4 (0.25, 0.50, 0.75, and 1.0) which are shown in Fig. 3, and the average contact angle shown in Fig. 4. Fig. 4 indicates that pure Psf has an average contact angle of 80.24°. Moreover, there is a trend that the water contact angle continues to decrease along with the increase in weight % of the addition of GO-Fe_3O_4 nanocomposites. The modified membrane water contact angle decreased from 79.01° to 73.17° (membrane with 0.75% GO-Fe_3O_4). The difference is that for a 1.0% addition of GO-Fe_3O_4, the membrane contact angle again increased to 75.92°. Furthermore, it increased more significantly than the standard membrane contact angle (Psf-pure) for GO/Psf membranes (86.09°). Therefore, the membrane that shows more hydrophilic properties has a composition of 0.75% GO-Fe_3O_4. This property is based on the interaction of the Fe-OH groups on the surface of the Fe_3O_4 material with water (H_2O) through strong hydrogen bonds, so adsorption is chemisorption [26].

The greater contact angle value is caused by the surface tension that occurs between the membrane and the water. In addition, there was a decrease in the interfacial energy between the hydrophilic Fe_3O_4 nanoparticle solution and the water/membrane during the phase inversion process [21]. However, generally, a small contact angle will result in better

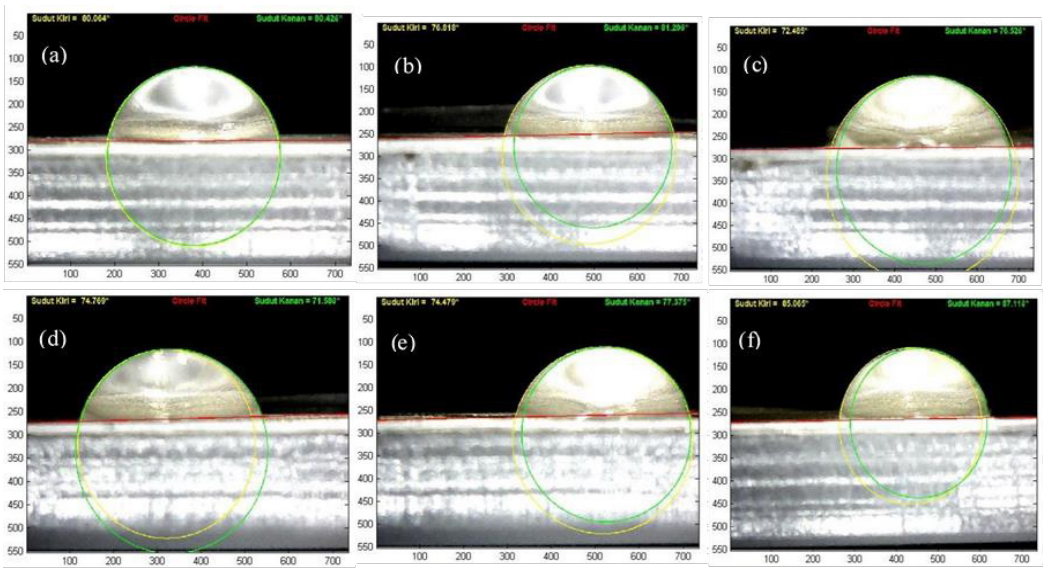

Fig. 3. The Contact angle of membranes: (a) Psf, (b-d) GO-Fe3O4/Psf untuk GO-Fe3O4 (%Wt): 0.25%, 0.50%, 0.75%, and 1.0%; and (f) GO (0.5%)/Psf

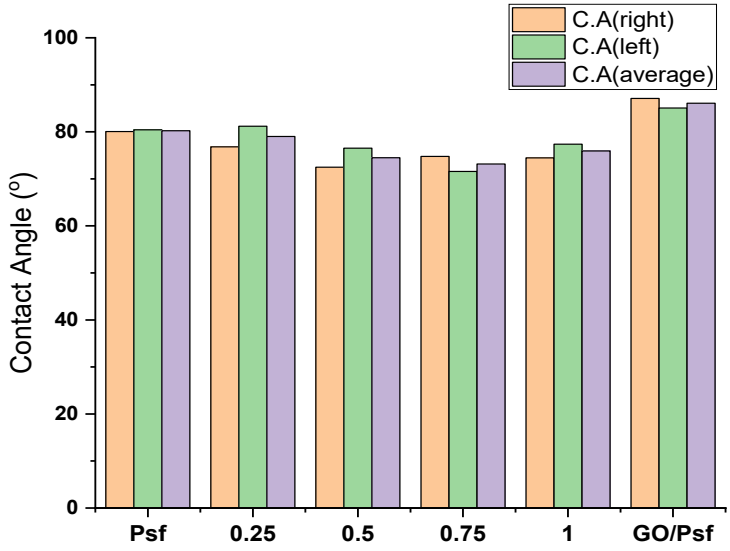

Fig. 4. The contact angle of membranes: Psf, GO-Fe_3O_4/Psf for GO-Fe_3O_4 0.25%, 0.50%, 0.75%, and 1.0%, respectively; and Fe_3O_4/Psf

hydrophilicity, increased water flux, and resistance to impurities [27]. Thus, the experimental results obtained in this study are by the literature [28].

Morphology of Graphene Membrane

The results of the scanning electron microscopy (SEM) test of the GO-Fe_3O_4 /PSF membrane are shown in Fig. 5. Fig. 5b shows a cross-sectional view of the modified composite membrane with topical asymmetrical morphology of the membrane fibers. The middle layer represents the predominant morphology with finger-like structures. This finger-like structure is characteristic of an asymmetrical membrane where the cross-section of the membrane consists of a finger structure with a porous underlayer [8]. The top layer of the GO- Fe_3O_4 /PSF membrane is the most porous compared to the PSf membrane alone. The formation of a porous surface on GO- Fe_3O_4 /PSF is caused by an increase in the hydrophilic nature

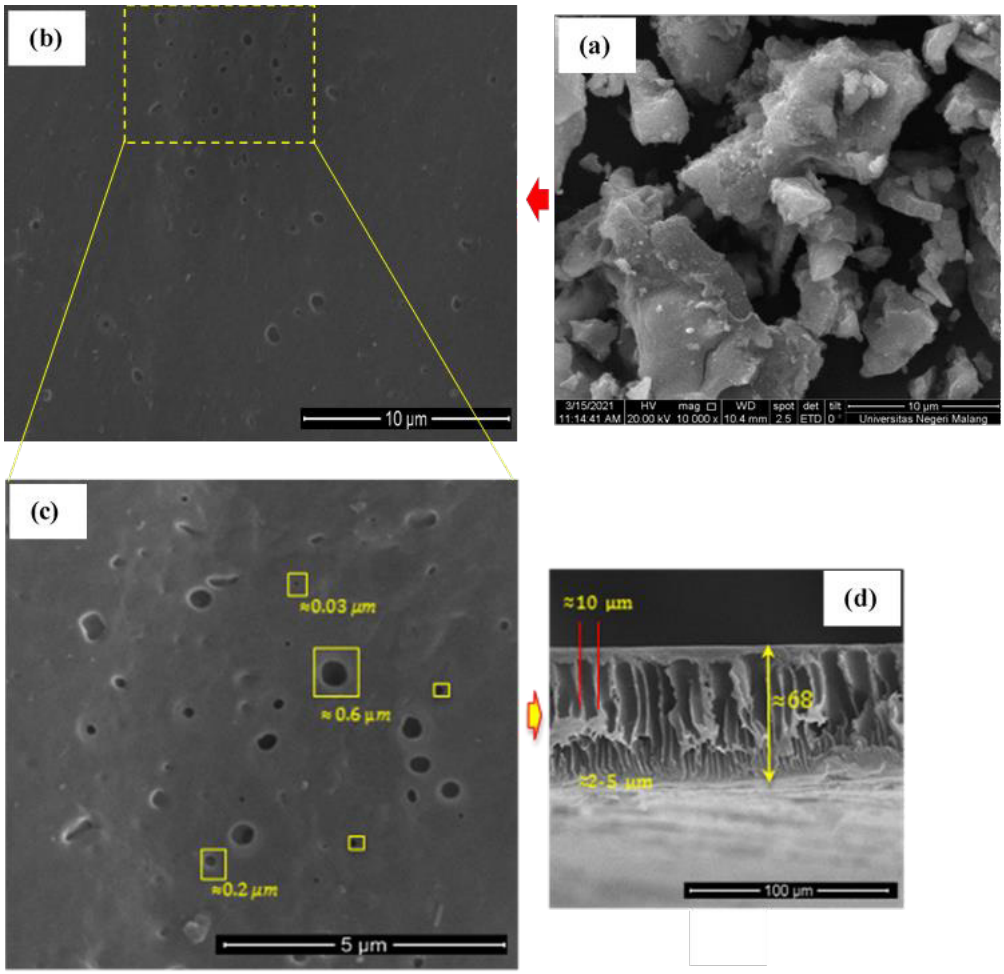

Fig. 5. Morphology of GO-Fe_3O_4 (0,75%) /PSf membrane: (a) GO-Fe_3O_4 Composite, (b-c) surface area, and (b) cross-secion.

of the solution which will accelerate the rate of solvent exchange [28]. The addition of Fe_3O_4 into the membrane causes a larger cavity. Theoretically, membrane permeability could increase in line with the number of macro-voids present [8].

From the results of the scanning electron microscopy test on the surface and cross-section of the GO-Fe_3O_4 /Psf membrane (shown in Fig. 5), it was found that there were pores in the membrane. The porous membrane could be seen clearly in Fig. 5(b). The thickness of the membrane is about 68 µm, with a pore diameter of about 2-10 µm (inside the membrane). The size of macro cavities such as fingers looks non-uniform, this is ascribed to the faster deposition of PES in contact with non-solvents (water). There are surface defects or holes formed during membrane preparation, causing the membrane cross-section to be inhomogeneous/ uniform in terms of size and distribution on the membrane surface (Fig. 5(a)). The addition of GO-Fe_3O_4 particles has a major effect on the formation of the membrane structure. They are, furthermore, shown in Fig. 4, the morphological profile of the GO/Psf membrane, where the frontal view (Fig. 6(a)) and the cross-sectional view (Fig. 6(b)). Compared with the GO-Fe_3O_4/Psf membrane, the number of pores and the width of the pores, the GO/Psf membrane is more numerous and broader. The presence of Fe_3O_4 nanoparticles narrows the membrane pores.

Salt Rejection of Graphene Membrane

The dyeing wastewater usually contains an appreciable quantity of salt, therefore it is of great importance to study the effect of salt on the separation performance of dye or salt mixtures. The salt rejection of the graphene membrane can inform the ability of a membrane to filter the salt

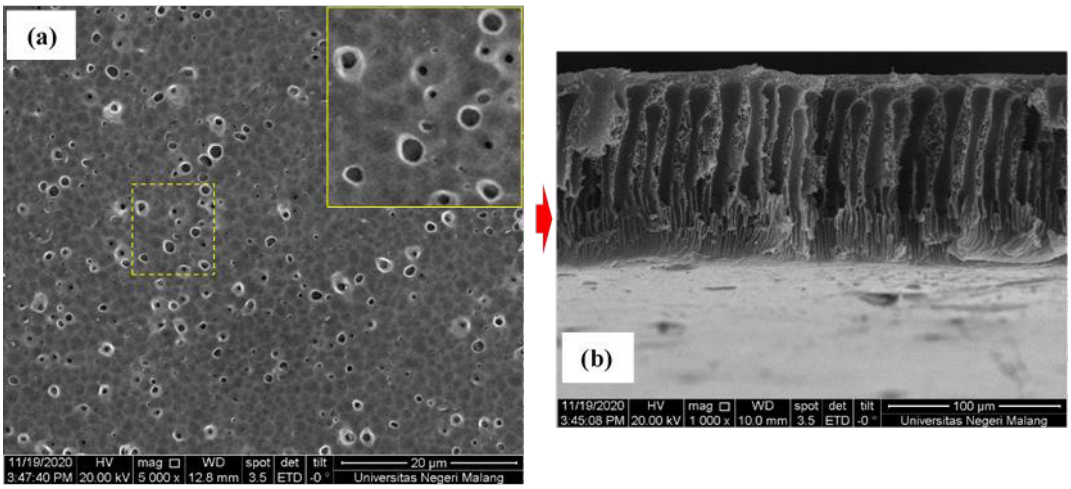

Fig. 6. Morphology of GO /PSf membrane: (a) surface and zoom (insert) and (b) cross-section.

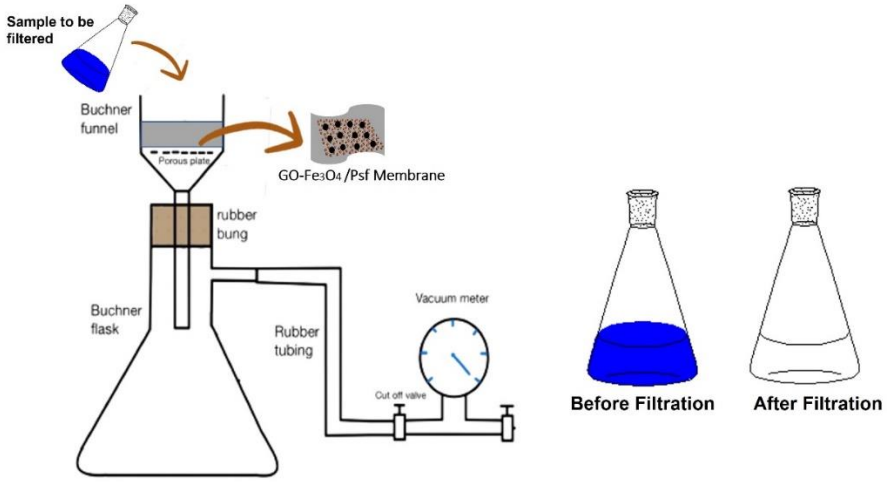

Fig. 7. The Filtration test with NaCl and MB

in the solution. A total of 10 ml of NaCl solution with a concentration of 27.79 g/mL was filtered using a device, as shown in Fig. 7. The membrane was weighed before use and later on filtered. The finished membrane is then dried and weighed.

The concentration of NaCl solution after filtration is calculated and later on, enters into the equation (1). The results of the salt-rejection calculation indicate that the GO-Fe_3O_4 membrane can be used for seawater desalination because the GO- Fe_3O_4 membrane can filter out NaCl compounds in the solution (Table 1).

The membrane with GO-Fe_3O_4 (0.25 wt.%) experienced a salt rejection of 45.88%, the membrane with GO- Fe_3O_4 (0.5 wt.%) experienced a salt rejection of 52.97%, the GO-Fe_3O_4 membrane (1.0%) experienced the salt rejection of 56.89%, GO membrane salt rejection of 42.35% was more significant than pure Psf membrane (32.92%). The best salt rejection occurred when filtering the NaCl solution using a membrane containing GO- Fe_3O_4 (0.75% wt.%), which was 59.33%. The increasing salt-rejection value indicates the denser the membrane pores, so the membrane's efficiency is also improving [29]. The best membrane efficiency is the membrane with GO-Fe_3O_4 content of 0.75%. For the rejection of NaCl, increased salt content leads to a higher concentration gradient near the membrane surface, which could facilitate the transport of NaCl through the membrane and thus

Table 1. Salt rejection of GO-Fe_3O_4/Psf membranes

GO-Fe_3O_4 (Wt%)/Psf membranes	*Cf*	*Cp*	*Salt-rejection (%)*
Psf-pure membrane	27.79	18.64	32.92
GO- Fe3O4 (0.25 %)		15.04	45.88
GO- Fe_3O_4 (0.50 %)		13.07	52.97
GO- Fe_3O_4 (0.75 %)		12.08	59.33
GO-Fe_3O_4 (1.00%)		11.98	56.89
GO/Psf membrane		16.02	42.35

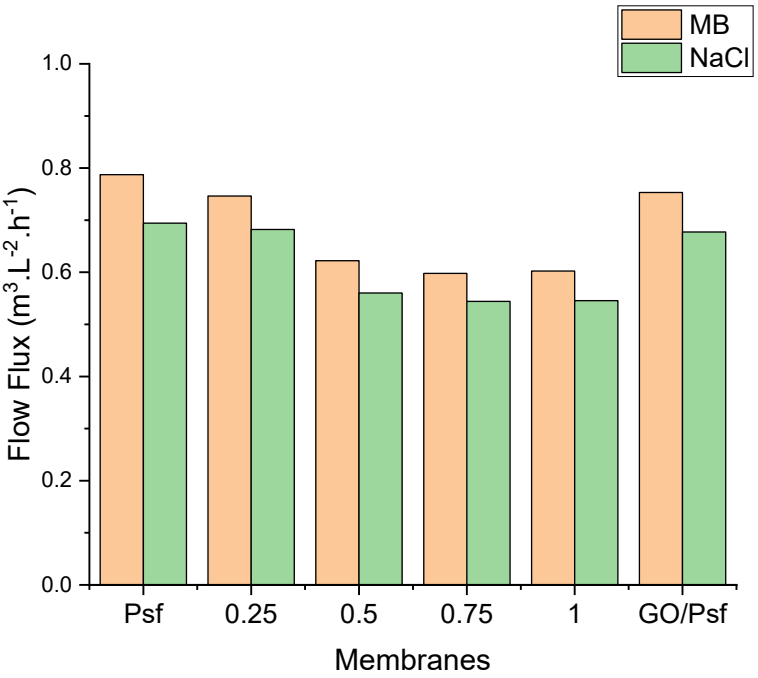

Fig. 8. Flow flux of methylene-blue and NaCl solution for GO- Fe_3O_4 /PFs membranes.

lower the rejection of NaCl [29]. Moreover, higher NaCl concentration can lower the electrostatic interaction of the charges in the membrane, and the membrane pores become thinner, which opens up the transport route of solutes through the membrane, allowing NaCl to pass through the membrane more easily [30]. The addition of Fe_3O_4 to the membrane was carried out to prevent the solute transport pathway through the membrane quickly and easily. In addition, GO-based membranes were reported to exhibit excellent desalination performance of the dye/salt mixture.

Flow Flux of Graphene Membrane

The presence of NaCl has a significant influence on the membrane flux. For example, the GO-Fe_3O_4 /Psf membrane flux continuously decreases from 81.63 $L.m^{-2}.h^{-1}$ to 62.79 $L.m^{-2}.h^{-1}$ with an increase of NaCl time from 0.11 hour to 0.15 hour, which is the result of the rise in osmotic pressure, concentration polarization, and dye adsorption into the membrane. The addition of GO- Fe_3O_4/Psf content in the membrane affects the value of the resulting flow flux (Fig. 8).

The filtering time of the methylene blue and NaCl solutions affects the value of the resulting water flux. The tighter the membrane pores make, the filtering time longer. The longest filtering time is using a membrane with a GO- Fe_3O_4 content of 0.75% because the membrane pores are denser, so the filtration process takes longer than other membranes. The higher flux value also indicates that the membrane has better fouling/dirty resistance [21].

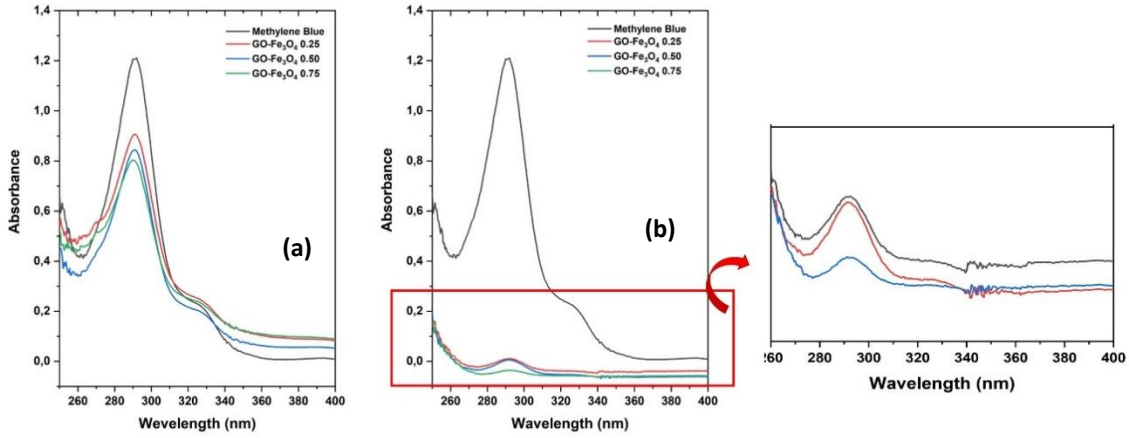

Fig. 9. UV-VIS of methylene blue filtration by GO- Fe_3O_4 /PSf membranes: (a) one-time and (b) fifth time.

The rejection ability of the dye and NaCl on the graphene membrane during the filtration process is shown in Fig. 8. A decrease in flow rate indicates the rejection of dye molecules and an increase in Na and Cl ions. Adding Fe3O4 nanoparticles to GO/Psf membranes increased their rejection performance compared to pure Psf membranes. The optimal composition for rejecting dyes and NaCl is a membrane composed of 0.75% GO-Fe_3O_4. GO/Psf membranes have good mechanical and thermal stability and are resistant to soiling while absorbing and repelling dye molecules efficiently through nanometer-sized pores; this is its advantage over pure Psf membranes [9], [31].

Graphene membrane is currently being developed for seawater desalination applications, where graphene membranes can be used to produce clean water from seawater by a filtration process. The mechanism of salt rejection in the graphene membrane occurs due to the interaction between the graphene membrane and salt ions in seawater. The mechanism of salt rejection in graphene membranes occurs through two processes, namely: the mechanism of salt rejection by the exclusion of pore size and the mechanism of salt rejection by the surface charge of the membrane [24], [31].

First: Adding Fe_3O_4 nanoparticles to graphene membranes could increase the efficiency and durability of the membrane in seawater desalination applications. The mechanism of NaCl rejection by graphene membranes that have been added Fe_3O_4 nanoparticles occurs through several processes, including the Salt rejection mechanism by pore size exclusion. As in graphene membranes without other nanoparticles, the mechanism of salt rejection in graphene membranes with other Fe_3O_4 nanoparticles occurs through pore size exclusion. Graphene membranes with Fe_3O_4 nanoparticles have tiny pores, so only water molecules and compounds with tiny molecular sizes can pass through. Therefore, salt with a molecular size larger than the pores of the graphene membrane cannot pass through it, resulting in a salt rejection process [32].

Second: Adding Fe_3O_4 nanoparticles to graphene membranes can also increase the surface charge of the membrane, thereby increasing the interaction between the surface charge of the membrane and salt ions in seawater. The surface of the graphene membrane that has been added with Fe_3O_4 nanoparticles will be more negatively charged, so it will be more effective in repelling salt ions which are also negatively charged. So that the salt ions contained in seawater cannot pass through the graphene membrane, and only water molecules and compounds with smaller molecular sizes can pass through its mechanism of salt rejection by adsorption of Fe_3O_4 nanoparticles. The Fe_3O_4 nanoparticles in the graphene membrane can selectively absorb salt ions, thereby increasing the effectiveness of salt rejection by the graphene membrane. Salt ions that pass through the membrane's pores will interact with the Fe_3O_4 nanoparticles and be adsorbed on the surface of the nanoparticles. So that salt ions cannot pass through the graphene membrane, and salt rejection occurs. With the addition of Fe_3O_4 nanoparticles

Table 2. Antimicrobial of GO-Fe_3O_4 compounds against E. coli and S. aureus

Bacterial	*Test Repeats*	*Inhibition zone diameter (cm) at various concentrations of GO- Fe_3O_4 compounds*				
		100 ppm	200 ppm	300 ppm	400 ppm	500 ppm
Escherichia coli	1	0.55	0.55	0.55	0.55	0.55
	2	0.55	0.55	0.55	0.55	0.55
	3	0.55	0.55	0.55	0.55	0.55
Staphylococcus aureus	1	0.55	0.55	0.55	0.55	0.55
	2	0.55	0.55	0.55	0.55	0.55
	3	0.55	0.55	0.55	0.55	0.55

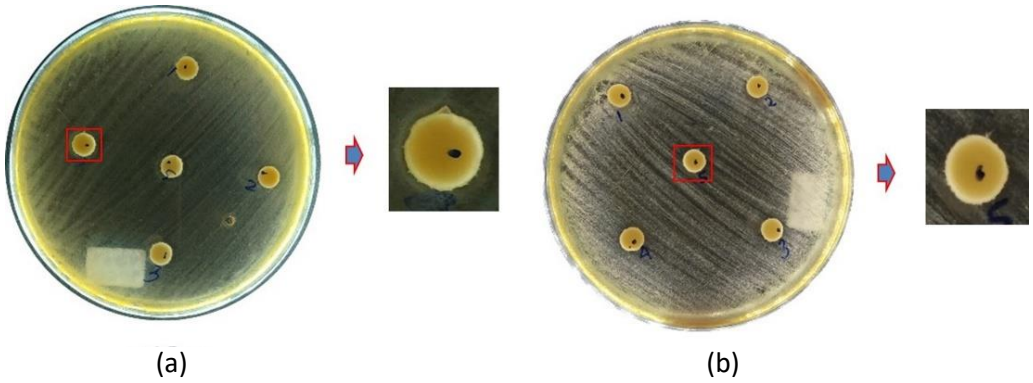

Fig. 10. Anti-Bacterial of GO- Fe_3O_4 /PSf: (a) E. Coli and (b) S. Aureus

to the graphene membrane, the NaCl rejection mechanism by the membrane will be more effective and efficient, thereby increasing the efficiency and durability of the membrane in seawater desalination applications [33].

Fig. 9(b) is a UV-VIS graph of methylene blue filtering five times. The resulting absorbance value is decreasing because more methylene blue is filtered. The decrease in the absorbance value of the methylene blue solution was caused by the less methylene blue content in the solution when it was filtered [16]. The membrane successfully filtered methylene blue. The membrane with GO-Fe_3O_4 content of 0.75% had the lowest absorbance than the membrane with GO-Fe_3O_4 0.5% and GO-Fe_3O_4 0.25%, which indicates that the membrane is more effective for water filtration.

Anti-Bacterial of GO-Fe_3O_4 /PSf Graphene Membrane

The anti-bacterial test was carried out using the disc diffusion method. Distilled water was used as a GO-Fe_3O_4 diluent, and the disc paper diameter was 0.55 cm. The disc diffusion test was carried out to determine the inhibition of the compound against bacterial growth. The bacterial suspension (OD600 nm 0.1) was rubbed on Muller Hinton Agar (MHA) media surface in Petri dishes using a sterile cotton swab. Paper disks containing 20 µl of the test compound were placed on the surface of the MHA. Incubation was carried out for 48 hours at 30°C. The clear zone formed around the disc was expressed as the inhibition of the compound against bacterial growth. Shown in Fig. 10. (a) is the inhibition of E-Coli bacteria, and in Fig. 10(b) is the inhibition zone against S. Aureus bacteria. The ability of inhibition against E. Coli and S. Aureus bacteria for all GO-Fe_3O_4 sample compositions (0.25%, 0.50%, and 0.75%) showed the same trend, marked with a clear/bright outer circle zone, which was 0.55 cm (Table 2).

The GO-Fe_3O_4 from Table 2 demonstrated good reproducibility, which is attributed to the fact that the surface was stable and maintained its ability to antimicrobial E. Coli and S. Aureus. The stability of compounds was investigated by repeating the test 3 times. The repetition multiple times to determine the characteristics of

Antimicrobial GO-Fe_3O_4 compounds against E. coli and S. aureus. The diameter areas suggested that the GO-Fe_3O_4 can attack the microbial target. All areas of concentration have the same effect on the entire area. Higher concentrations of GO-Fe_3O_4 do not provide a statistically significant impact, as evidenced by the concentration ranges (ppm). Using a minor concentration (ppm) to observe a considerable shift from this result is preferable. Anti-bacterial tests are needed to support that this graphene-based membrane material is perfect for application as a filtration material in filtration equipment systems to obtain safe water for consumption [34], [35].

CONCLUSION

In this study, the GO-Fe_3O_4/Psf membrane was successfully synthesized using the inversion method. The addition of GO- Fe_3O_4 material into the Psf membrane (0.25%, 0.50%, 0.75%, and 1.00%) has been carried out. The results indicated that the membrane containing GO- Fe_3O_4 0.75% by weight had the highest salt rejection value (59.33%) with the lowest flow flux, the flow flux value was 62.79 for methylene-blue solution and 54.42 $L.m^{-2}.h^{-1}$ for NaCl solution. The membrane with 0.75% GO- Fe_3O_4 content had the longest filtering time because the membrane pores were tighter. A different thing happened for membranes with 1.00% GO- Fe_3O_4 content, it was suspected that there was over content and there was an accumulation of GO- Fe_3O_4 particles on the Psf polymer layer. The GO- Fe_3O_4/Psf membrane was also tested for anti-bacterial using E. Coli and S. Aureus bacteria. Aureus by disc diffusion method. The results showed good reproducibility, this was related to the fact that the addition of GO- Fe_3O_4 to the membrane made the surface stable and maintained its ability to anti-bacterial E. Coli and S. Aureus.

ACKNOWLEDGEMENT

The author would like to thank the Faculty of Mathematics and Natural Sciences, Universitas Negeri Surabaya (Unesa), for supporting laboratory facilities and funding through this collaborative research. Thanks to the Department of Physics, Universiti Negeri Malang (UM), and the Department of Physics, Universitas Teknologi Malaysia (UTM).

CONFLICT OF INTEREST

The authors hereby declare that there is no conflict of interest.

REFERENCES

[1] E. K. Sijabat, A. Nuruddin, P. Aditiawati, and B. S. Purwasasmita, "Synthesis and Characterization of Bacterial Nanocellulose from Banana Peel for Water Filtration Membrane Application," J. Phys.: Conf. Ser., vol. 1230, no. 1, p. 012085, Jul. 2019, doi: 10.1088/1742-6596/1230/1/012085. https://doi.org/10.1088/1742-6596/1230/1/012085

[2] A. Balasubramanian, "Properties of Seawater-Documentary," 2011, doi: 10.13140/RG.2.2.14014.48969.

[3] S. Koushkbaghi, P. Jafari, J. Rabiei, M. Irani, and M. Aliabadi, "Fabrication of PET/PAN/GO/Fe 3 O 4 nanofibrous membrane for the removal of Pb (II) and Cr(VI) ions," Chemical Engineering Journal, vol. 301, pp. 42-50, Oct. 2016, doi: 10.1016/j.cej.2016.04.076. https://doi.org/10.1016/j.cej.2016.04.076

[4] H. H. I. Eltigani and Y. Boonyongmaneerat, "Progress of water desalination applications based on wettability and surface characteristics of graphene and graphene oxide: A review," J Met Mater Miner, vol. 32, no. 3, pp. 15-26, Sep. 2022, doi: 10.55713/jmmm.v32i3.1520. https://doi.org/10.55713/jmmm.v32i3.1520

[5] H. K. Hassan, N. J. Al-Amiri, and M. M. Yassen, "Desalination Technology of Water by using Rice Husk Ash," BJAS, vol. 27, no. 2, pp. 148-160, Dec. 2014, doi: 10.33762/bagrs.2014.111805. https://doi.org/10.33762/bagrs.2014.111805

[6] H. Zheng, Solar energy desalination technology. Amsterdam, Netherlands: Elsevier, 2017.

[7] P. V. Chai, J. Y. Law, E. Mahmoudi, and A. W. Mohammad, "Development of iron oxide decorated graphene oxide (Fe3O4/GO) PSf mixed-matrix membrane for enhanced antifouling behavior," Journal of Water Process Engineering, vol. 38, p. 101673, Dec. 2020, doi: 10.1016/j.jwpe.2020.101673. https://doi.org/10.1016/j.jwpe.2020.101673

[8] T. D. Kusworo et al., "Simultaneous Photocatalytic and Membrane Filtration Using Graphene Oxide (Go)/Sio2 Composite for Enhanced Removal of Organic Pollutant and Ammonia from Natural Rubber-Laden Wastewater," SSRN Journal, 2022, doi: 10.2139/ssrn.4017566. https://doi.org/10.2139/ssrn.4017566

[9] C. Pui Vun, A. W. Mohammad, T. Yeit Haan, and E. Mahmoudi, "Evaluation of Iron Oxide Decorated On Graphene Oxide (Fe3O4/GO) Nanohybrid Incorporated in Psf Membrane At Different Molar Ratios for Congo Red Rejection," Jurnal Teknologi, vol. 79, no. 1-2, Jan. 2017, doi: 10.11113/jt.v79.10440. https://doi.org/10.11113/jt.v79.10440

[10] P. V. Chai, E. Mahmoudi, Y. H. Teow, and A. W. Mohammad, "Preparation of novel polysulfone-Fe3O4/GO mixed-matrix membrane for humic acid rejection," Journal of Water Process Engineering, vol. 15, pp. 83-88, Feb. 2017, doi: 10.1016/j.jwpe.2016.06.001. https://doi.org/10.1016/j.jwpe.2016.06.001

[11] Y. Huang, C. Xiao, Q. Huang, H. Liu, J. Hao, and L. Song, "Magnetic field induced orderly arrangement of Fe3O4/GO composite particles for preparation of Fe3O4/GO/PVDF membrane," Journal of Membrane Science, vol. 548, pp. 184-193, Feb. 2018, doi: 10.1016/j.memsci.2017.11.027.

https://doi.org/10.1016/j.memsci.2017.11.027
[12] L. Huang, P. Zhu, G. Li, D. (Daniel) Lu, R. Sun, and C. Wong, "Core-shell SiO 2 @RGO hybrids for epoxy composites with low percolation threshold and enhanced thermo-mechanical properties," J. Mater. Chem. A, vol. 2, no. 43, pp. 18246-18255, Sep. 2014, doi: 10.1039/C4TA03702B. https://doi.org/10.1039/C4TA03702B
[13] Munasir and A. Terraningtyas, "Synthesis and characterization of Fe3O4/SiO2 composite with in-situ method: TEOS as SiO2 NPs precursor," J. Phys.: Conf. Ser., vol. 1171, p. 012050, Feb. 2019, doi: 10.1088/1742-6596/1171/1/012050. https://doi.org/10.1088/1742-6596/1171/1/012050
[14] M. Nasir, R. P. Kusumawati, D. H. Kusumawati, A. Taufiq, and D. Darminto, "Characterization of Fe3O4/rGO Composites from Natural Sources: Application for Dyes Color Degradation in Aqueous Solution," IJE, vol. 33, no. 1, Jan. 2020, doi: 10.5829/ije.2020.33.01a.03. https://doi.org/10.5829/ije.2020.33.01a.03
[15] Munasir, A. Taufiq, Ambarwati Teraningtyas, Diah Hari Kusumawati, and Zainul Arifin Imam Supardi, "Nanosized Fe3O4/SiO2 core-shells fabricated from natural sands, magnetic properties, and their application for dye adsorption," Engineering and Applied Science Research, vol. 49, p. 340352, 2022, doi: 10.14456/EASR.2022.35.
[16] A. Fernández-Pérez and G. Marbán, "Visible Light Spectroscopic Analysis of Methylene Blue in Water; What Comes after Dimer," ACS Omega, vol. 5, no. 46, pp. 29801-29815, Nov. 2020, doi: 10.1021/acsomega.0c03830. https://doi.org/10.1021/acsomega.0c03830
[17] N. P. Putri, D. H. Kusumawati, N. Widiyanti, and Munasir, "Synthesis of polyaniline/cellulose composite as humidity sensor," J. Phys.: Conf. Ser., vol. 997, p. 012009, Mar. 2018, doi: 10.1088/1742-6596/997/1/012009. https://doi.org/10.1088/1742-6596/997/1/012009
[18] Munasir and R. P. Kusumawati, "Synthesis and Characterization of Fe3O4@rGO Composite with Wet-Mixing (ex-situ) Process," J. Phys.: Conf. Ser., vol. 1171, p. 012048, Feb. 2019, doi: 10.1088/1742-6596/1171/1/012048. https://doi.org/10.1088/1742-6596/1171/1/012048
[19] Y. A. B. Neolaka et al., "The adsorption of Cr(VI) from water samples using graphene oxide-magnetic (GO-Fe3O4) synthesized from natural cellulose-based graphite (kusambi wood or Schleichera oleosa): Study of kinetics, isotherms and thermodynamics," Journal of Materials Research and Technology, vol. 9, no. 3, pp. 6544-6556, May 2020, doi: 10.1016/j.jmrt.2020.04.040. https://doi.org/10.1016/j.jmrt.2020.04.040
[20] Z. Han et al., "A review of performance improvement strategies for graphene oxide-based and graphene-based membranes in water treatment," J Mater Sci, vol. 56, no. 16, pp. 9545-9574, Jun. 2021, doi: 10.1007/s10853-021-05873-7. https://doi.org/10.1007/s10853-021-05873-7
[21] V. M. Alfianti, M. Munasir, and Department of Physics, Universitas Negeri Surabaya, "Fabrication and Characterization of GO-Fe3O4/PSF Membrane with Phase Inversion Method," JPSE, vol. 6, no. 2, pp. 55-60, Jul. 2021, doi: 10.17977/um024v6i22021p055. https://doi.org/10.17977/um024v6i22021p055
[22] W. C. M. Henkens and J. A. M. Smit, "Salt rejection and flux in reverse osmosis with compactible membranes," Desalination, vol. 28, no. 1, pp. 65-85, Jan. 1979, doi: 10.1016/S0011-9164(00)88127-8. https://doi.org/10.1016/S0011-9164(00)88127-8
[23] M. W. Hakami, A. Alkhudhiri, S. Al-Batty, M.-P. Zacharof, J. Maddy, and N. Hilal, "Ceramic Microfiltration Membranes in Wastewater Treatment: Filtration Behavior, Fouling and Prevention," Membranes, vol. 10, no. 9, p. 248, Sep. 2020, doi: 10.3390/membranes10090248. https://doi.org/10.3390/membranes10090248
[24] T. A. Agbaje, S. Al-Gharabli, M. O. Mavukkandy, J. Kujawa, and H. A. Arafat, "PVDF/magnetite blend membranes for enhanced flux and salt rejection in membrane distillation," Desalination, vol. 436, pp. 69-80, Jun. 2018, doi: 10.1016/j.desal.2018.02.012. https://doi.org/10.1016/j.desal.2018.02.012
[25] B. Jaleh, E. S. Etivand, B. F. Mohazzab, M. Nasrollahzadeh, and R. S. Varma, "Improving Wettability: Deposition of TiO2 Nanoparticles on the O2 Plasma Activated Polypropylene Membrane," IJMS, vol. 20, no. 13, p. 3309, Jul. 2019, doi: 10.3390/ijms20133309. https://doi.org/10.3390/ijms20133309
[26] N. Barati, M. M. Husein, and J. Azaiez, "Modifying ceramic membranes with in situ grown iron oxide nanoparticles and their use for oily water treatment," Journal of Membrane Science, vol. 617, p. 118641, Jan. 2021, doi: 10.1016/j.memsci.2020.118641. https://doi.org/10.1016/j.memsci.2020.118641
[27] J. Guo, M. U. Farid, E.-J. Lee, D. Y.-S. Yan, S. Jeong, and A. Kyoungjin An, "Fouling behavior of negatively charged PVDF membrane in membrane distillation for removal of antibiotics from wastewater," Journal of Membrane Science, vol. 551, pp. 12-19, Apr. 2018, doi: 10.1016/j.memsci.2018.01.016. https://doi.org/10.1016/j.memsci.2018.01.016
[28] M. Mosayebi, Z. Salehi, H. Doosthosseini, P. Tishbi, and Y. Kawase, "Amine, thiol, and octyl functionalization of GO-Fe3O4 nanocomposites to enhance immobilization of lipase for transesterification," Renewable Energy, vol. 154, pp. 569-580, Jul. 2020, doi: 10.1016/j.renene.2020.03.040. https://doi.org/10.1016/j.renene.2020.03.040
[29] N. M. Chauke, R. M. Moutloali, and J. Ramontja, "Development of ZSM-22/Polyethersulfone Membrane for Effective Salt Rejection," Polymers, vol. 12, no. 7, p. 1446, Jun. 2020, doi: 10.3390/polym12071446. https://doi.org/10.3390/polym12071446
[30] A. Al-Asmar, C. V. L. Giosafatto, M. Sabbah, A. Sanchez, R. Villalonga Santana, and L. Mariniello, "Effect of Mesoporous Silica Nanoparticles on The Physicochemical Properties of Pectin Packaging Material for Strawberry Wrapping," Nanomaterials, vol. 10, no. 1, p. 52, Dec. 2019, doi: 10.3390/nano10010052. https://doi.org/10.3390/nano10010052
[31] H. Jee et al., "Enhancing the Dye-Rejection Efficiencies and Stability of Graphene Oxide-Based Nanofiltration Membranes via Divalent Cation Intercalation and Mild Reduction," Membranes, vol. 12, no. 4, p. 402, Apr. 2022, doi: 10.3390/membranes12040402. https://doi.org/10.3390/membranes12040402
[32] A. Aghigh, V. Alizadeh, H. Y. Wong, Md. S. Islam, N. Amin, and M. Zaman, "Recent advances in utilization of graphene for filtration and desalination of water: A review," Desalination, vol. 365, pp. 389-397, Jun. 2015, doi: 10.1016/j.desal.2015.03.024. https://doi.org/10.1016/j.desal.2015.03.024
[33] A. Anand, B. Unnikrishnan, J.-Y. Mao, H.-J. Lin, and C.-C. Huang, "Graphene-based nanofiltration

membranes for improving salt rejection, water flux and antifouling-A review," Desalination, vol. 429, pp. 119-133, Mar. 2018, doi: 10.1016/j.desal.2017.12.012. https://doi.org/10.1016/j.desal.2017.12.012

[34] A. Lee, J. W. Elam, and S. B. Darling, "Membrane materials for water purification: design, development, and application," Environ. Sci.: Water Res. Technol., vol. 2, no. 1, pp. 17-42, 2016, doi: 10.1039/C5EW00159E. https://doi.org/10.1039/C5EW00159E

[35] G. Memisoglu, R. C. Murugesan, J. Zubia, and A. G. Rozhin, "Graphene Nanocomposite Membranes: Fabrication and Water Treatment Applications," Membranes, vol. 13, no. 2, p. 145, Jan. 2023, doi: 10.3390/membranes13020145. https://doi.org/10.3390/membranes13020145